Experimental method for the assessment of agricultural spray retention based on high-speed imaging of drop impact on a synthetic superhydrophobic surface

Mathieu Massinon, Frédéric Lebeau*

Unité de Mécanique et Construction, Département des Sciences et Technologies de l'Environnement, University of Liege – Gembloux Agro-Bio Tech
Passage des Déportés, 2, B-5030 Gembloux, Belgium
*E-mail: f.lebeau@ulg.ac.be, tel: +32 (0) 81 62 21 65, fax: +32 (0) 81 62 21 67

Abstract

Spray retention is a critical stage in pesticide application since non-retained drops results in reduced efficacy, economic loss and environmental contamination. Current methods of retention assessment are based either on field experiments or laboratory studies. The former are usually performed on whole plants under realistic spray application conditions but offer no insight into the physics behind the process whilst the latter mainly focus on drop impact physics but are usually restricted to unrealistically low drop speeds. The aim of the paper is to devise an experimental method to investigate retention at drop scale level as a function of operational parameters but under controlled realistic conditions. A device based on high-speed video was developed to study retention on a synthetic superhydrophobic surface for a moving agricultural nozzle. The sizes and velocities of drops generated were measured immediately before impact using image analysis. Impact class proportions were established and transition boundaries between impact outcomes were quantified using Weber number. Two contrasting experiments were performed to investigate the ability of method to detect small parametric changes. The insignificant changes in spray pattern that occur from pressure changes, did not significantly affect impact class boundaries, but changed the proportion of drops in each class because of size and velocity variations. The use of a surfactant reduced the volume mean diameter of the spray, increased impact speed and changed the impact class boundaries. The method should allow a precise parametric investigation of spray retention in laboratory and close to field conditions.

Keywords: Spray retention, Drop impact, Weber number, Moving agricultural nozzle, Superhydrophobicity.

1. Introduction

Pesticide application efficiency improvement is required for health, safety, environmental and cost considerations. Zabkiewicz (2007) divided the measurement of the spray application process in 4 individual stages, namely *deposition*, defined as the amount deposited in the target area; *retention*, the fraction of drops captured by plant; *uptake*, the fraction of the retained material taken up into plant foliage and *translocation*, the amount of absorbed material translocated from absorption site. Depending on the scenario, it was estimated that the efficiency of the deposition process was in the 80 to 95 % range whilst the retention process was in the 10 to 100% range, resulting in a combined worst case efficiency of 8%. Much research has therefore been devoted to minimise these losses, either by improvements in spray technology or the physicochemical properties of the pesticide formulation, the objective being to decrease the amount of chemical applied per unit area whilst ensuring that the dose of chemical required for control reaches the target.

Some spray application studies focus on deposition and retention as a whole at plant scale. Butler Ellis et al. (2004) examined the effect of liquid properties and application technology on spray retention in a range of situations representative of practical pesticide application. Retention on whole plants was strongly influenced both by plant growth and plant canopy. Changes in pesticide application method from conventional flat-fan to air induction nozzle had a detrimental effect. Leaf surface was influenced by age and growing conditions with indoor grown plants being more difficult-to-wet than outdoor grown plants due to leaf surface abrasion. Lower dynamic surface tension (DST) of the spray mixture improved retention, especially when using an air induction nozzle on difficult-to-wet leaves. These results show that retention process is governed by numerous factors: drop size and velocity, physicochemical properties of spray formulation, spatial distribution within the canopy and target surface properties. This approach provided an integrated estimate of the deposition and retention but failed to develop a fundamental understanding of the physics behind the processes.

Some research has focussed on the retention phase at the drop scale. Drop impact was then studied using imaging devices and drop generators (Yang et al., 1991). This approach was used by Foster et al. (2005) to devise a statistical model based on extensive experimental work to predict the adhesion/bounce transition. The parameters or combination of parameters used were the product of velocity and drop diameter, leaf angle, leaf surface and formulation surface tension. Shattering is not usually observed in these studies. Monodisperse drops were produced, using either on demand or continuous drop generators (Reichard, 1998). On demand droplet generators are restricted to generating drops at their terminal velocities at best and a single drop is produced at a time. Continuous drop generators have the advantage to produce higher speed drops but they are however limited in size by the orifice diameter and aerodynamic interactions with the surrounding air (Sirignano and Mehring, 2000).

While an overall approach to measurement can highlight the effects of nozzle drop size spectra, measurements at drop scale fail to produce drop size and velocity distributions representative of agricultural nozzles. However, both approaches highlight the major influence of leaf wettability on the retention process. Wettability refers to the drop behaviour on the leaf surface. The diversity of plant and their surface structures led a wide range of wetting, from superhydrophilic to superhydrophobic (Koch and Barthlott, 2009). Gaskin et al. (2005) proposed a method to rank plant surfaces using acetone-water contact angle measurements. Easy-to-wet leaves retain most of the drops while difficult-to-wet ones, such as blackgrass or wheat, are difficult to treat. More particularly, the hydrophobic behaviour of leaves usually originates from their waxy cuticles. If the leaf coating is composed of hydrophobic crystal waxes that generate small-scale roughness, this may result in superhydrophobicity (Taylor, 2011). Unfortunately, because of the variability of superhydrophobic natural leaf surfaces, retention studies face reproducibility limitations. When comparisons of small operational variations such as changes in pressure or adjuvants are conducted, serious limitations on sensitivity may result.

Manufacturers are interested in clarifying the relationship between pesticide application methods and the physicochemical properties of the pesticide formulation and spray retention to guide their technical developments. To support this objective, a theoretical review that links drop dynamics and impact outcome for superhydrophobic surfaces is presented. Using this theoretical basis, an assessment method is proposed to analyse the physics of drop retention at the drop scale under controlled and realistic conditions. A synthetic superhydrophobic surface is used to perform tests on a well-controlled target representative of difficult-to-wet leaves. Experiments performed at different operating pressures and surfactant concentrations were used to assess the performance of the method.

2. Theoretical background

Drop impact on superhydrophobic surfaces is considered in this section as the foundation for further work. The aim is to deliver the connections between drop properties, wettability and impact behaviours on a superhydrophobic surface.

A drop hitting a surface exhibits different behaviours depending on drop size and velocity, liquid and surface properties. However, each impact begins with the same steps. The drop then spreads until it reaches its maximum spreading diameter. Different options are possible depending on the surface wetting regime and the drop energy during impact.

Two models describe the wetting of superhydrophobic surfaces depending on the liquid surface tension (Zu et al., 2010; Taylor, 2011). The Wenzel non-composite regime (Wenzel, 1936), often referred as pinning, is characterised by the adhesion of the liquid which is anchored in the surface cavities. The liquid expels the trapped air below the drop if the liquid surface tension is sufficiently low to allow the liquid to penetrate into the surface roughness. In the Cassie-Baxter composite regime (Cassie and Baxter, 1944), the liquid standing on the pillars of the surface traps air in the valleys of the structure. Therefore, the liquid can be easily removed from the surface. Both models relate apparent contact angle with the surface roughness. A relevant roughness parameter is the Wenzel roughness which is defined as the ratio of the real and the projected planar surface areas (Rioboo et al., 2008). However, this parameter is not necessarily sufficient to forecast the transition between wetting regimes because pinning is dependent on topography. The effect of height and distance between the pillars are currently being studied (Zu et al., 2010) to give better prediction of the wetting than the traditional models.

Dimensional analysis has been classically used to investigate the relationship between variables involved in the retention process (Lake and Marchant, 1983; Rein, 1993). The relevant dimensionless parameter governing the drop-surface interaction in absence of viscosity modification is the Weber number ($We = \rho v^2 d / \sigma$) of the drop. It represents the ratio between the kinetic energy and the surface energy, where ρ is liquid density, v is the drop velocity before impact, d is the drop diameter and σ is liquid static surface tension. Other relevant dimensionless parameters in the dynamics of drop impact are the Reynolds number ($\mathrm{Re} = \rho v d / \mu$) where μ is the dynamic viscosity, and the Ohnesorge number ($Oh = \sqrt{We} / \mathrm{Re} = \mu / \sqrt{\rho \sigma d}$) which is relevant if viscosity varies.

Different impact outcomes have been identified on superhydrophobic materials as a function of drop size and velocity and surface roughness (Fig. 1). For small roughness, a drop of low Weber number adheres in a Wenzel state. The static contact angle is small. As Weber number increases, a part of the drop can bounce, in what is referred to as partial rebound. At higher Weber number a drop can be shattered into several satellite drops, with a part of the drop adhered to the impact point, in what is referred to as pinning fragmentation. At intermediate roughness, low velocity drops adhere in a Cassie-Baxter regime. With increasing speed, the drop rebounds but this can only be observed on superhydrophobic surfaces under the Cassie-

Baxter regime (Richard and Quéré, 2000) if the receding contact angle is sufficiently high (Rioboo et al., 2008). For even greater speeds, when the impact pressure is sufficiently large, the liquid can penetrate into the cavities of the surface modifying the wettability regime from Cassie-Baxter to Wenzel regimes (Tsai et al., 2011). As a consequence, sticking, partial rebound or pinning fragmentation can occur. Finally, for higher roughness, a drop can, as a function of speed, either be deposited in a Cassie-Baxter regime, rebound or completely splash. In the latter case, the expending film is lifted and leads to a rim disintegration caused by hydrodynamic instabilities (Range and Feuillebois, 1998; Šikalo et al., 2002). The reasons for the fundamental instability of splashing, currently explained either by a Rayleigh-Taylor or Kelvin-Helmholtz instability, are still under discussion (Park et al., 2008).

Extensive work has be carried out on the physical understanding of impact on superhydrophobic surfaces (Bartolo et al., 2006; Reyssat et al., 2006) as well as impact modelling (Caviezel et al., 2008) and promising robust physical models have emerged from these theoretical advances (Taylor, 2011). As instance, Rioboo et al. (2008) proposed a constant Weber number as boundary between impact outcomes in their experiments on porous superhydrophobic surface using distilled water. Mercer et al. (2010) and Forster et al. (2010) proposed transition models based on a combination of dimensionless numbers to account the range of liquid used in pesticide application.

3. Materials and method

3.1. Dynamic spray application bench (Fig. 2)

Drops were generated by a flat-fan nozzle XR11003VK (Spraying Systems Co, Wheaton, IL, USA) mounted on a height-adjustable boom sprayer. Spray mixture was pressurised and mixed in a 10 l stainless steel tank. A precision pressure gage was placed at the nozzle level to be independent of any pressure drop in supply pipes. Fluid intake was controlled by a solenoid valve. Nozzle height was set at 500 mm above the target. A single passage of the nozzle was performed for each test. A linear displacement stage, actuated by a servomotor, moved the nozzle at a forward speed of 2 m s^{-1} perpendicular to the camera-lighting axis. Different techniques for measurement of drop size and velocity distributions have used static nozzles (Tuck et al., 1997). It was however shown that spray deposits below a nozzle differs between static and moving nozzles because of the modified air entrainment process (Lebeau, 2004).

Drop impacts were recorded using a high-speed camera (Y4 CMOS, Integrated Design Tools, Tallahassee, FL, USA) using backlighting to maximise the contrast. The acquisition frequency was set at 20,000 images per second to ensure a good identification and characterisation of drop impacts. Shutter time was set to 9 µs with a +3dB sensor gain to get an average background grey level of roughly 200, with an 8 bit pixel depth. An optical system (12X zoom system, Navitar, Rochester, NY, USA) gave a 10.58 µm.$pixel^{-1}$ spatial resolution, depth of field at about 2 mm and working distance at 341 mm. A background correction was performed before tests with embedded camera software (Motion Studio, Integrated Design Tools, Tallahassee, FL, USA) providing an homogeneous image. Sensing triggered the camera recording. A LED lighting (19-LED Constellation, Integrated Design Tools, Tallahassee, FL, USA) with a beam angle of 12.5° placed 500 mm behind the target surface provided both high illumination and uniform background to the images. The lighting was used in a pulsed mode and triggered by the image acquisition.

A horizontal slit plate (Fig. 3) was placed 10 mm above the surface to select drops that are in the focal plane. Slit width was smaller than the camera depth of field. The measurement zone was about 2 mm height by 10 mm long. The linear translation stage was used to adjust the target position in the camera focal plane. In this configuration, drop size and velocity can be measured just before impact. No secondary drops resulting from a splashing or a rebound that occurred out of the focal plane were taken into account in the analysis. A completely PTFE coated microscope blade (part number X2XES2013BMNZ, Thermo Fisher Scientific Inc., Waltham, MA, USA) was used in experiments. A static contact angle of 169° (sessile drop method, 5 replicates, CAM200, KSV Instruments, Helsinki, Finland) for a 5 µl distilled water drop characterises water repellent surface. The relevance of the use of this superhydrophobic surface as target surface has been studied in comparison with outdoor grown wheat leaves (Massinon and Lebeau, 2012) using this method.

3.2. Size and velocity measurements

The size and velocity of drops was determined in a two stage process. Firstly, in a manual screening phase, acquired images were viewed by an operator who encoded the frame number corresponding to the onset of a new drop in the upper part of the scene (Fig. 4A) and a second frame was noted when the drop was located just above the surface, before impact (Fig. 4B). As a result, the displacement of the drop between the two selected images is kept to around 1 mm for high accuracy speed measurements for slower drops. The operator also identified and recorded the impact type (as defined in section 2) based on subsequent frames (Figs. 4C to 4F). These data were stored in a text file. In the second phase, selected images are screened by an image analysis procedure developed in Matlab (The MathWorks® Company, Natick, MA, USA). The first operation consisted of identifying and filling the objects in the image for a fixed threshold, followed by labelling. Once objects were identified, an equivalent diameter was computed using a corresponding circle with the same area as the drop. This was to take into account the non-spherical shape of the drops. The latter procedure was successively applied using two close segmentation thresholds to check on drop image sharpness. If the difference between diameters obtained for each threshold was greater than 10 µm, the drop was considered to be out of focus and was not taken into account for the further processing. Drop velocity was computed as the module of the vector defined by the difference in position between the drop centres between the two selected frames divided by the elapsed time. If multiple drops were found on the same image, the operator was prompted to select successive images or ones of interest. As a result a matrix of impact events was generated. It contained drop size and velocity, computed Weber number, impact type and frame number. Considering a ± 20 µm uncertainty in the distance between drop centres, the accuracy in the calculated velocity was a maximum of 2% at 8 m s^{-1}. Maximum uncertainty in drop diameter measurement was 10 µm.

Once drop size and velocity were determined, results were summarised in graphical form depending on drop size and velocity. Transitions were determined using a constant Weber number as boundary. The Weber number of transition was determined by the intersection between Weber number probability density distributions of the different impact outcomes. A drop of the Weber number of transition has an equal probability of belonging to different classes. In the log-log graphs of velocity versus diameter, a constant Weber number of transition corresponds to a straight line with a -0.5 slope. Finally, volumetric proportions of the spray in each class were computed and retention was assessed.

3.3 Experiments

Two experiments were performed to examine how the system can be used to assess spray retention and point out advantages and limitations of the method. In the first experiment, three spray pressures (0.2, 0.3 and 0.4 MPa) were used with distilled water. In the second experiment, a trisiloxane surfactant (Break Thru S240®, Evonik Industries AG, Essen, Germany) was tested at three concentrations in distilled water: 0.025, 0.05 and 0.1% (V/V) at 0.3 MPa spray pressure.

4. Results and discussion

4.1. Effect of pressure on retention (experiment 1)

Graphical outputs of the method for distilled water are presented in Figs. 5, 6 and 7 for 0.2, 0.3 and 0.4 MPa spray pressure respectively. Overall, coarse drops with higher velocities were completely shattered into satellites drops (fragmentation, +). Intermediately sized drops, with diameters from roughly 100 µm to 300 µm bounced off the surface (rebound, ●). Finally, fine drops with low velocity were directly adhered on the surface (adhesion, Δ). Adhesion refers to sticking both in Wenzel or Cassie-Baxter regime in this paper. Two clouds of points could be distinguished on these figures. The sigmoid-shaped cloud corresponds to primary impact. It represented the size and velocity distributions before impact resulting from sheet breakup, transport and evaporation of each drop. The second cloud of points, located below the latter, corresponds to secondary impacts. They originated from a rebound or a pinning rebound (○). The drops present a Cassie-Baxter wetting regime during impact, except for pinning rebound events for which the liquid undergoes a transition from Cassie-Baxter to Wenzel. A pressure increase leads to the production of more drops below 100 µm diameter. These small drops hit the target at a slightly higher velocity than their terminal velocity. They are found in the third cloud above the first impact cloud. The reason for this is the more energetic liquid sheet breakup (Sirignano and Mehring, 2000) due to increased pressure; this is confirmed by the decrease of the volumetric median diameter (VMD) (Table 1). The VMD statistic indicates the diameter with half the spray volume is contained in droplets that were smaller than this value. Another hypothesis could be that a VMD decrease leads to an increase in induced airflow. More numerous and smaller drops exchange more momentum with surrounding air which induces a stronger downward airflow and a slightly higher impact velocity. The VMD decrease was also associated with a higher proportion of deposited drops. The proportion of splashing reached a maximum at 0.3 MPa spray pressure and then decreased at 0.4 MPa because there are simply less coarse drops.

On Figs 5, 6 and 7, two limits are identified corresponding to adhesion/rebound boundary (A/R) and rebound/fragmentation boundary (R/F). The limits were determined using a constant Weber number (*We*) as described in section 3.2. All the $We_{A/R}$ are pressure independent (Table 1). However differences between $We_{R/F}$ originate from the small number of observed drops characterised by a Weber numbers close to $We_{R/F}$. The limit should not be assessed using a single Weber number, but by defining a range of Weber numbers as a function of contact angle hysteresis (Rioboo et al., 2008).

Overall, the increase of initial energy has no detrimental effect on retention in these conditions. Splashing is reduced and adhesion is increased because of big drop proportion depletion and small drop proportion increase. The increase of primary adhesion may however have a drastic effect on treatment efficacy, for instance on small or low LAI (Leaf Area Index) target such as those encountered in black-grass weeding.

4.2. Effect of surfactant concentration on retention (experiment 2)

Figures 8, 9 and 10 present phase diagrams of impact outcomes for three surfactant concentrations: 0.025, 0.05 and 0.1 (% V/V) respectively. At first glance, surfactant reduces the rebound. This effect is more pronounced as the surfactant concentration increases. These observations are corroborated with a gradual reduction of rebound proportion and decrease of the VMD (Table 1) as highlighted by Butler Ellis et al. (2001). For 0.1 (% V/V) concentration bouncing even disappears on this surface (Fig. 10). At this concentration, the surfactant allows the liquid to expel the air located into surface cavities and to penetrate deeply inside the surface matrix (Taylor, 2011). The mixture is therefore able to undergo a Cassie-Baxter to Wenzel regime transition and no rebound is observed anymore. The splashing threshold decrease to a Weber number of 95 calculated with static surface tension. However, timescale for drop impact is very low and depends essentially on drop size (Richard et al., 2002), so a dynamic surface tension would be more suited in the Weber number calculation. For instance the contact time for a 100 µm drop is about 0.5 ms which may be too short to allow the adsorption of the surfactant onto the new interface. Accordingly a drop containing lower surfactant concentration can still bounce despite the low static surface tension. Surfactant concentration effect during splashing is observable at the solid-liquid interface, the central part of the drop sticking at the surface because of transition to Wenzel regime at this level. The splashing is therefore modified to a pinning fragmentation (×) as a substantial part of the drop adheres on the surface. As a consequence, a better characterisation of splashing is needed in further investigations to estimate the fraction of the drop that disintegrates in small drops from the part sticking to the surface.

5. Conclusions

A measurement method of spray retention using both high-speed imaging and a superhydrophobic surface is proposed. The main interests are in the integration of all variables involved in a single trial, the production of realistic drop distributions leading to the onset of all impact types and the use of dimensionless number to forecast transitions between the impact outcomes.

On the basis of the conducted experiments, the method can highlight the effect of any modification of operational parameters on retention. Pressure modification affects retention by changing proportions in the different impact classes. The modification of the mixture surface tension affected the spray characteristics before impact as well as impact types and boundaries. The rebound progressively vanished with the increase of surfactant concentration. Splashing energy threshold is not highly modified but a pinning fragmentation appears because of Cassie-Baxter to Wenzel transition, what needs further investigations for precise quantification.

The method can be extended to investigate the effect of other parametrical changes such as the impact angle, spray height or nozzle kind. The use of a superhydrophobic reference guarantees the reproducibility of the trials and allows an overall ranking of the efficiency of application techniques and additives. The characterisation of natural leaf surface properties as well as liquid properties such as DST and polymeric additives (Bergeron, 2003) are promising research areas for the setup.

Acknowledgements

This research is funded by the Walloon public service DG06 (Belgium) in the frame of the EUREKA (http://www.eurekanetwork.org) project 4984 VEGEPHY.

References

Bartolo, D., Bouamrirene, F., Verneuil, É., Buguin, A., Silberzan, P. and Moulinet, S. (2006). Bouncing or sticky drops: Impalement transitions on superhydrophobic micropatterned surfaces, *Europhysics Letters*, 74 (2), 299-305.

Bergeron, V. (2003). Designing intelligent fluids for controlling spray applications, *C.R. Physique*, 4, 211-219.

Butler Ellis, M.C., Tuck, C.R. and Miller, P.C.H. (2001). How surface tension of surfactant solutions influences the characteristics of sprays produced by hydraulic nozzles used for pesticides application, *Colloids and Surfaces A: Physicochemical and Engineering Aspects*, 180, 267-276.

Butler Ellis, M.C., Webb, D.A. and Western, N.M. (2004). The effect of different spray liquids on the foliar retention of agricultural sprays by wheat plants in a canopy, *Pesticide Management Science*, 60, 786-794.

Cassie, A.B. and Baxter, S. (1944). Wettability of porous surfaces, *Transactions of the Faraday Society*, 40, 546-551.

Caviezel, D., Narayanan, C. and Lakehal, D. (2008). Adherence and bouncing of liquid drops impacting on dry surfaces, *Microfluid Nanofluid*, 5, 469-478.

Forster, W.A., Kimberley, M.O. and Zabkiewicz, J.A. (2005). A universal spray drop adhesion model, *Transactions of the ASABE*, 48(4), 1321-1330.

Forster, W.A. Mercer, G.N. and Schou, W.C. (2010). Process-driven models for spray droplet shatter, adhesion or bounce. *Proceedings of the 9th International Symposium on Adjuvants for*

Agrochemicals. ed. P Baurand M Bonnet. Technical University of Munich, Freising, Germany, 277-285.

Gaskin, R.E., Steele, K.D. and Forster,W.A. (2005). Characterising plant surfaces for spray adhesion and retention, *New Zeland Plant Protection*, 58, 179-183.

Koch, K. and Barthlott, W. (2009). Superhydrophobic and superhydrophilic plant surfaces: an inspiration for biomimetic materails, *Philosophical Transactions of The Royal Society A*, 367, 1487-1509.

Lake, J.R., Marchant, J.A. (1983). The use of dimensional analysis in a study of drop retention on barley, *Pesticide Science*, 14 (6), 638-644.

Lebeau, F. (2004). Modelling the dynamic distribution of spray deposits, *Biosystems Engineering*, 89 (3), 255-265.

Massinon, M. and Lebeau, F. (2012). Comparison of spray retention on synthetic superhydrophobic surface with retention on outdoor grown wheat leaves, *Aspects of Applied Biology* 114, *International Advances in Pesticide Application*, 261-268.

Mercer, G.N., Sweatman, W.L., Elvin, A., Caunce, J., Fulford, G. and Harper, G. (2007). Process driven models for spray retention in plants. In: Wake G, editor. Proceedings of the 2006 Mathematics in Industry study group, 57–85.

Park, H., Yoon, S.S., Jepsen, R.A., Heister, S.D. and Kim, H.Y. (2008). Drop bounce simulations and air pressure effects on the deformation of pre-impact drops, using a boundary element method, *Engineering Analysis with Boundary Elements*, 32, 21-31.

Range, K. and Feuillebois, F. (1998). Influence of surface roughness on liquid drop impact, *Journal of colloid and interfacial science*, 203, 16-30.

Reichard, D.L., Cooper, J.A., Bukovac, M.J. and Fox, R.D. (1998). Using a videographic system to assess spray drop impaction and reflection from leaf and artificial surfaces, *Pesticide Science*, 53 (4), 291-299.

Rein, M. (1993). Phenomena of liquid drop impact on solid and liquid surfaces. *Fluid Dynamics Research*, 12, 61-93.

Reyssat, M., Pépin, A., Marty, F., Chen, Y. and Quéré, D. (2006). Bouncing transitions on microtextured materials, *Europhysics Letters*, 74 (2), 306-312.

Richard, D. and Quéré, D. (2000). Bouncing water drops, *Europhysics Letters*, 50 (6), 769-775.

Richard, D., Clanet, C. and Quéré, D. (2002). Contact time of a bouncing drop, *Nature*, 417, 811.

Rioboo, R., Voué, M., Vaillant, A. and De Coninck, J. (2008). Superhydrophobic surfaces from various polypropylenes, *Langmuir*, 24 (17), 14074-14077.

Šikalo, Š., Marengo, M., Tropea, C. and Ganić, E.N. (2002). Analysis of impact of drops on horizontal surfaces, *Experimental Thermal and Fluid Science*, 25, 503-510.

Sirignano, W.A. and Mehring, C. (2000). Review of theory of distortion and disintegration of liquid streams, *Progress in Energy and Combustion Science*, 26 (4-6), 609-655.

Taylor, P. (2011). The wetting of leaf surface, *Current opinion in colloid and interface science*,16(4), 326–334.

Tsai, P., Hendrix, M. H. W., Dijkstra, R. R. M., Shui, L. & Lohse, D. (2011). Microscopic structure influencing macroscopic splash at high Weber number. *Soft Matter*, 7, 11325-11333.

Tuck, C.R., Ellis, M.C.B., and Miller, P.C.H. (1997). Techniques for measurement of drop size and velocity distributions in agricultural sprays, *Crop Protection*, 16 (7), 619-628.

Wenzel, R.N. (1936). Resistance of solid surface to wetting by water, *Industrial & Engineering Chemistry*, 28(8), 988-994.

Yang, X., Madden, L.V., Reichard, D.L., Fox, R.D. and Ellis, M.A. (1991). Motion analysis of drop impaction on a strawberry surface, *Agricultural and Forest Meteorology*, 56, 67-92.

Zabkiewicz, J.A. (2007). Spray formulation efficacy-holistic and futuristic perspectives, *Crop Protection*, 26, 312-319.

Zu, Y. Q., Yan, Y. Y., Li, J. Q. & Han, Z. W. (2010), Wetting Behaviours of a Single Droplet on Biomimetic Micro Structured Surfaces, *Journal of Bionic Engineering*, 7 (2), 191-198.

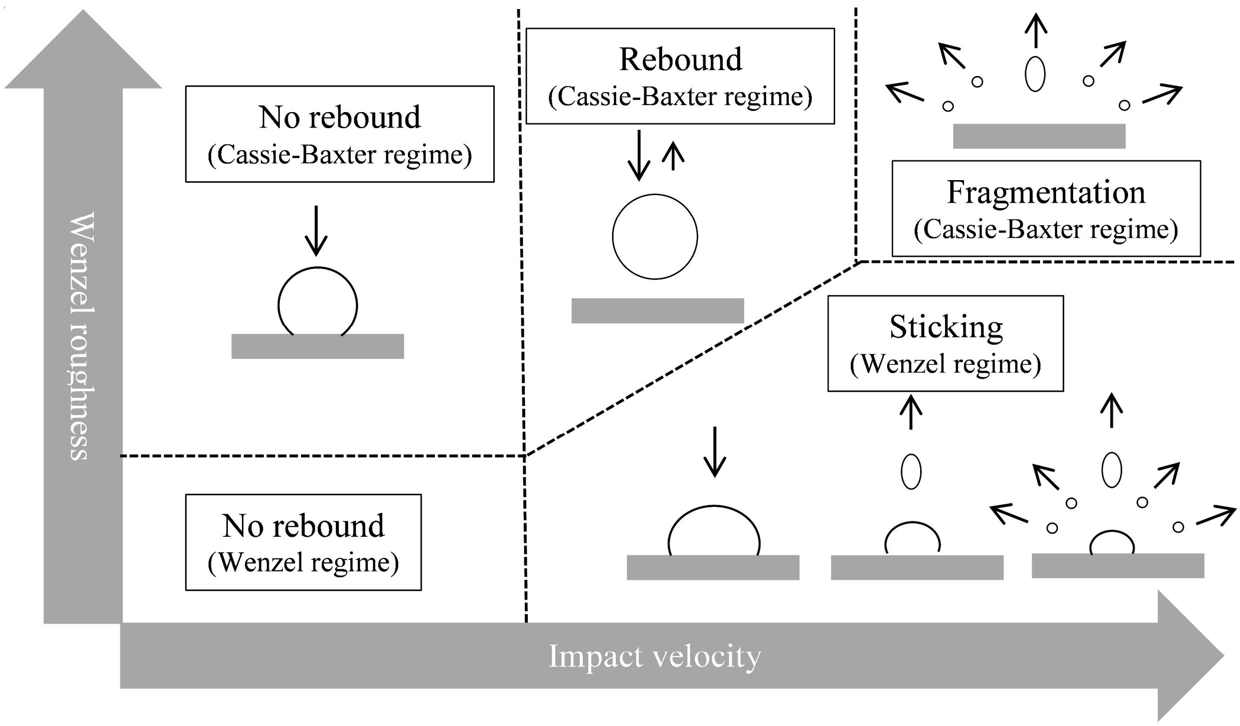

Fig. 1: Impact map for a drop depending on Wenzel roughness and drop impact velocity (from Rioboo et al., 2008).

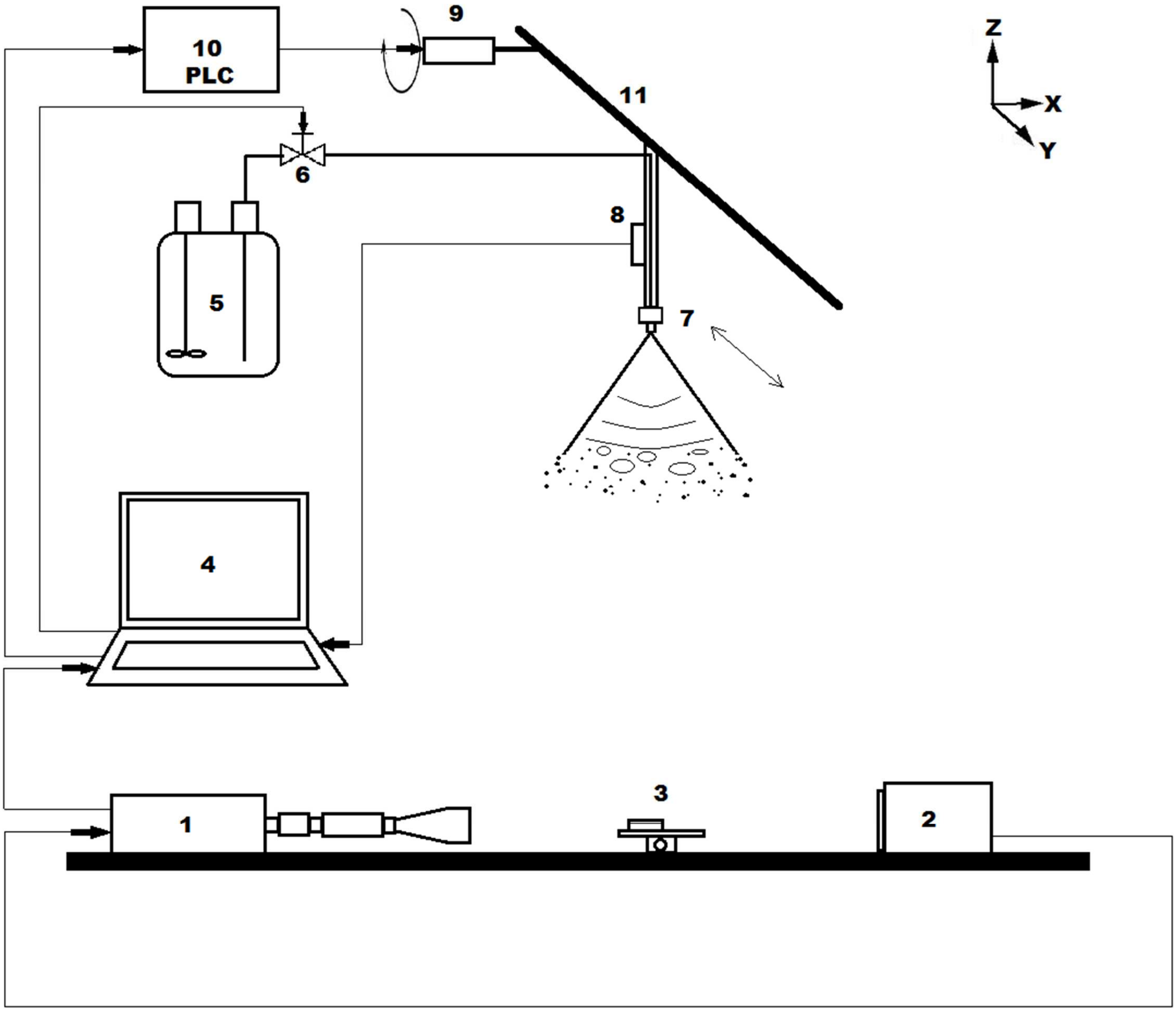

Fig. 2: Dynamic spray application bench: (1) high-speed camera, (2) LED lighting, (3) target surface on linear stage, (4) computer, (5) pressurised tank, (6) solenoid valve, (7) nozzle, (8) pressure gage, (9) servomotor, (10) programmable controller, (11) linear stage.

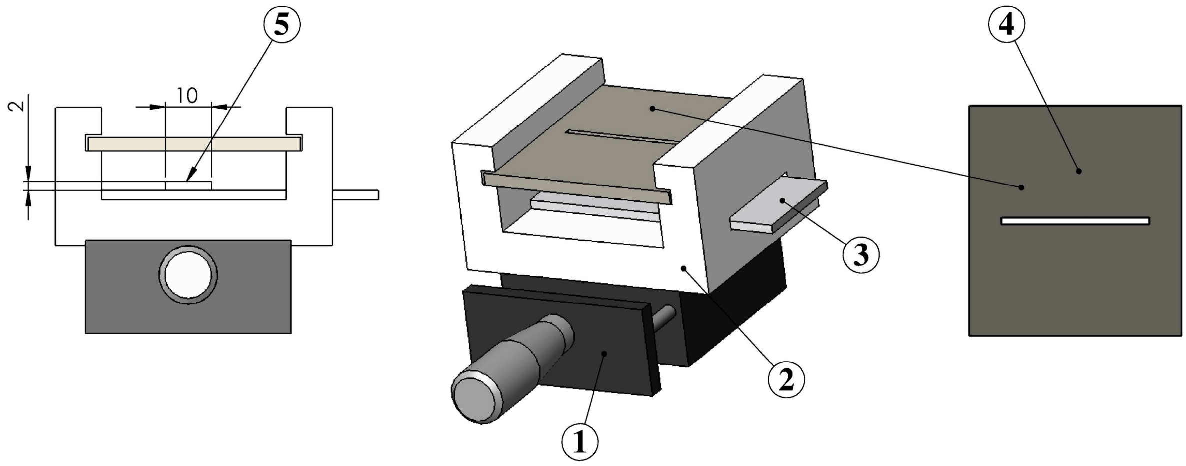

Fig. 3: Target bracket: (1) linear stage, (2) blade holder, (3) superhydrophobic target surface, (4) slit plate (slit width corresponds to 1.5 mm camera depth of field), (5) measurement area corresponding to the image size (10 mm length on 2 mm height).

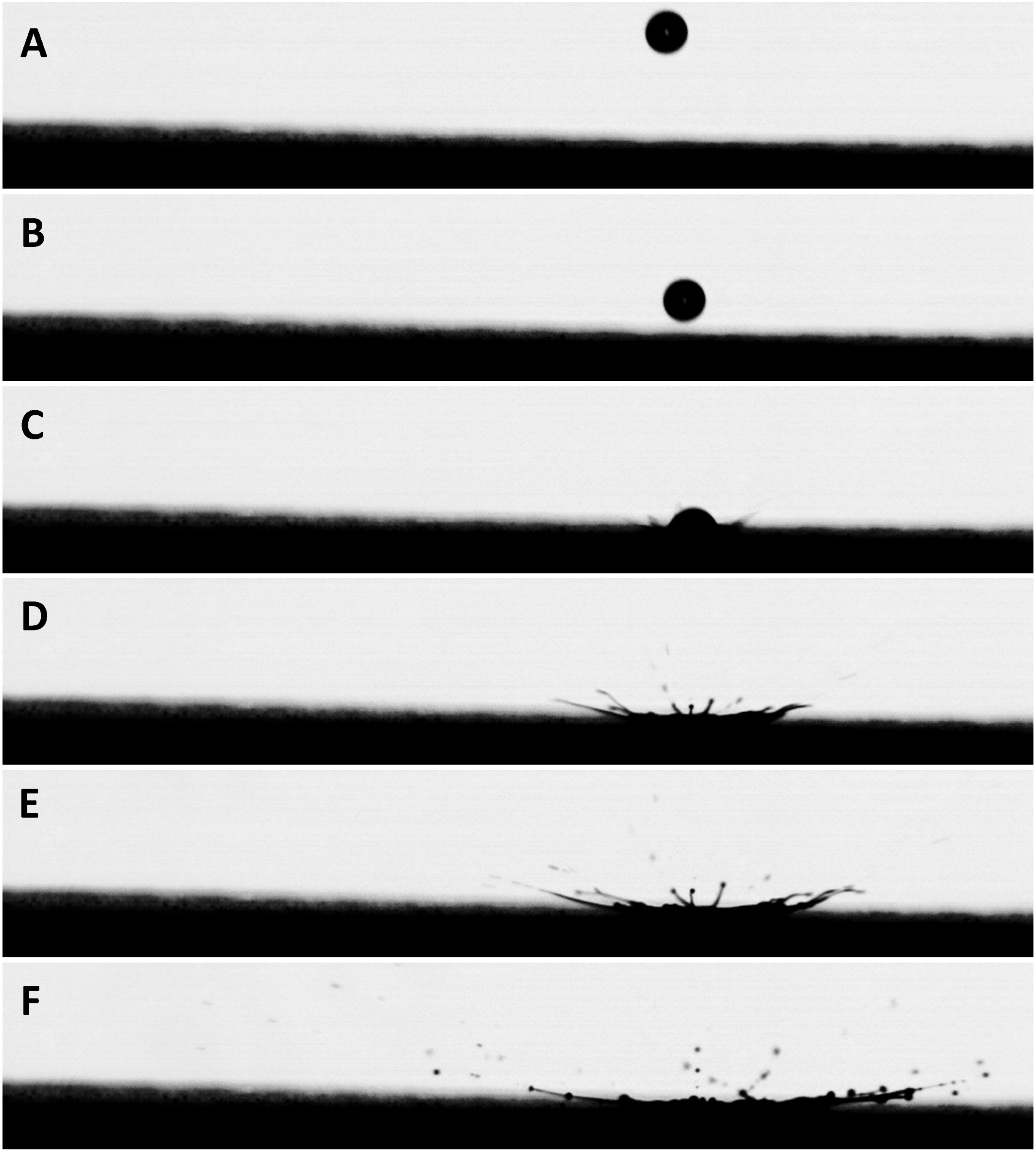

Fig. 4: (A-F): Impact of a drop on the superhydrophobic blade. (A, B) Images used for the determination of speed and diameter by image analysis, (C-F) images used by the operator to determine impact type.

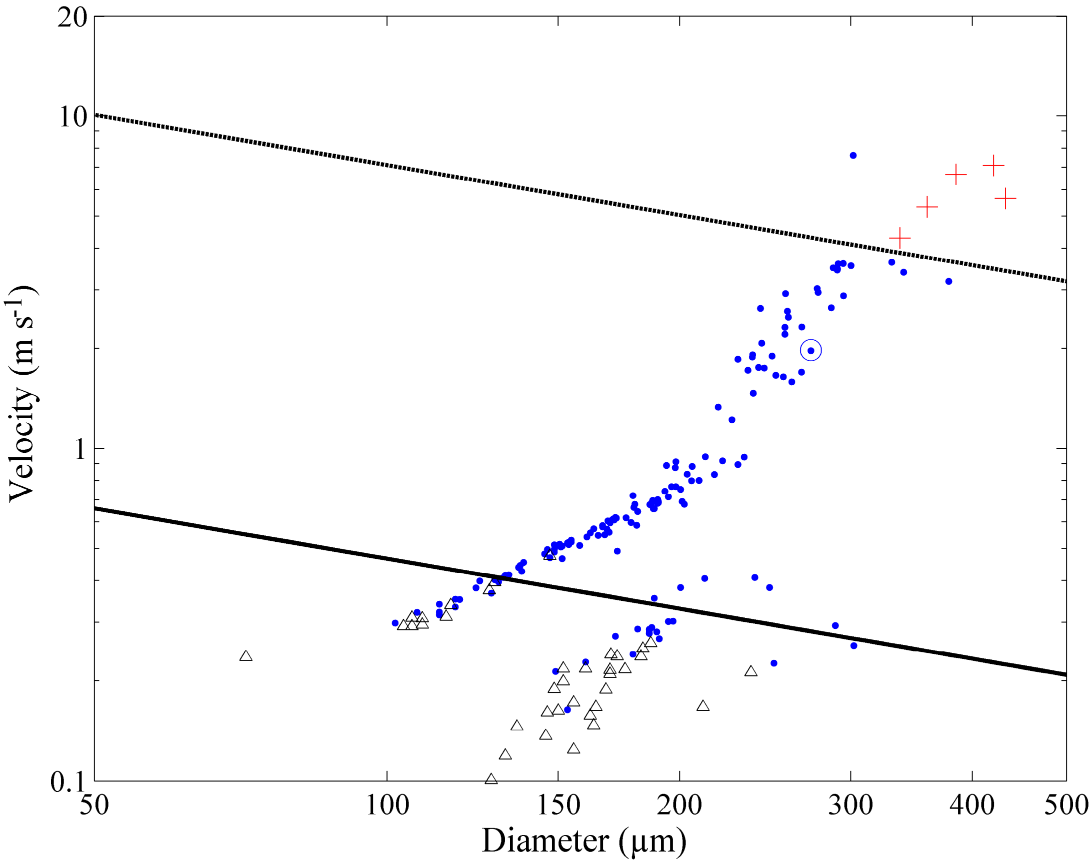

Fig. 5: Impact outcomes on the superhydrophobic slide for distilled water at 0.2 MPa (Teejet 11003 nozzle at 0.5 m height): Δ adhesion, ● rebound, ○ pinning rebound, + complete fragmentation, —— Weber number of transition between adhesion and rebound (*We* = 0.3), - - - Weber number of transition between rebound and fragmentation (*We* = 70).

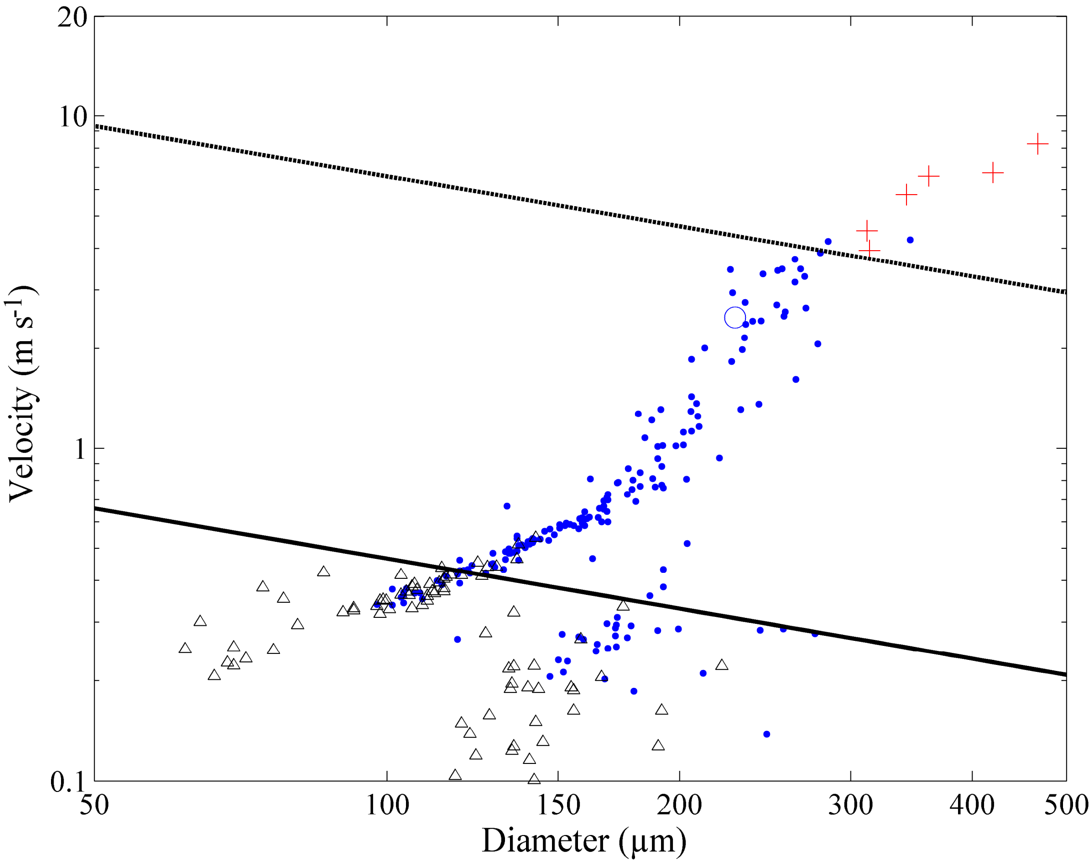

Fig. 6: Impact outcomes on the superhydrophobic slide for distilled water at 0.3 MPa (Teejet 11003 nozzle at 0.5 m height): Δ adhesion, ● rebound, ○ pinning rebound, + complete fragmentation, —— Weber number of transition between adhesion and rebound (*We* = 0.3), - - - Weber number of transition between rebound and fragmentation (*We* = 60).

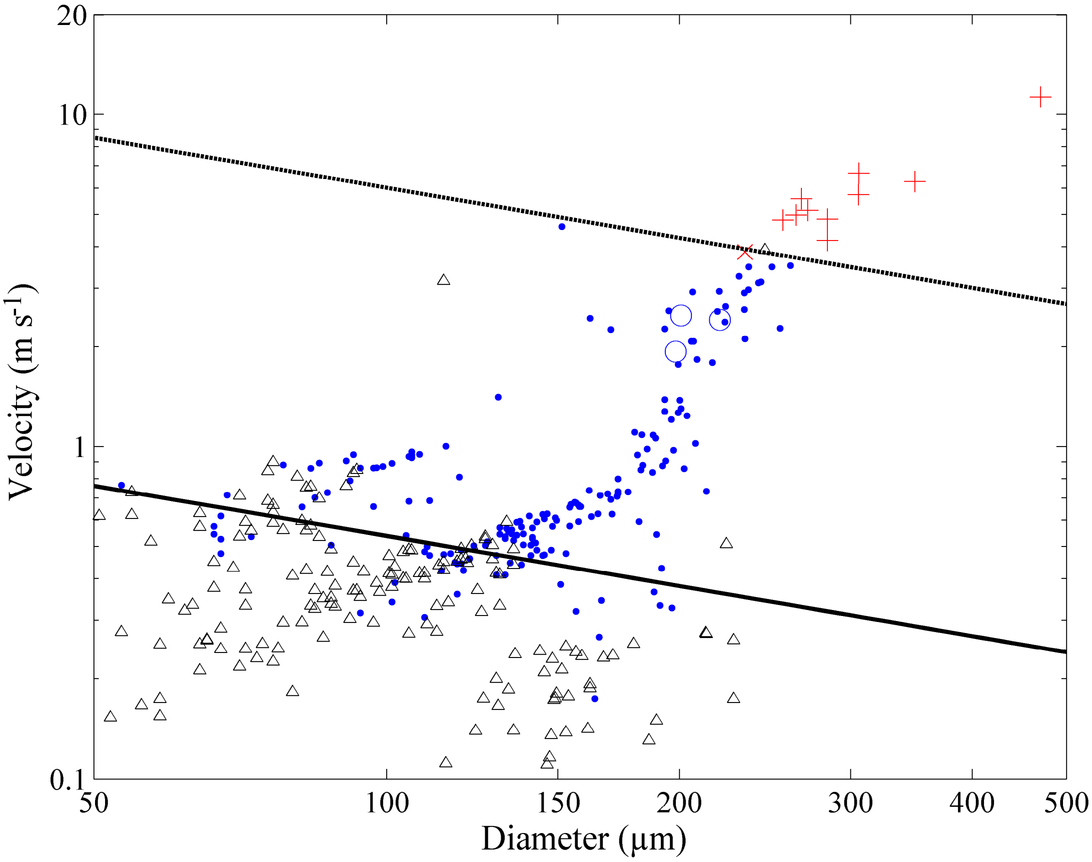

Fig. 7: Impact outcomes on the superhydrophobic slide for distilled water at 0.4 MPa (Teejet 11003 nozzle at 0.5 m height): Δ adhesion, ● rebound, ○ pinning rebound, × pinning fragmentation, + complete fragmentation, —— Weber number of transition between adhesion and rebound (*We* = 0.4), - - - Weber number of transition between rebound and fragmentation (*We* = 50).

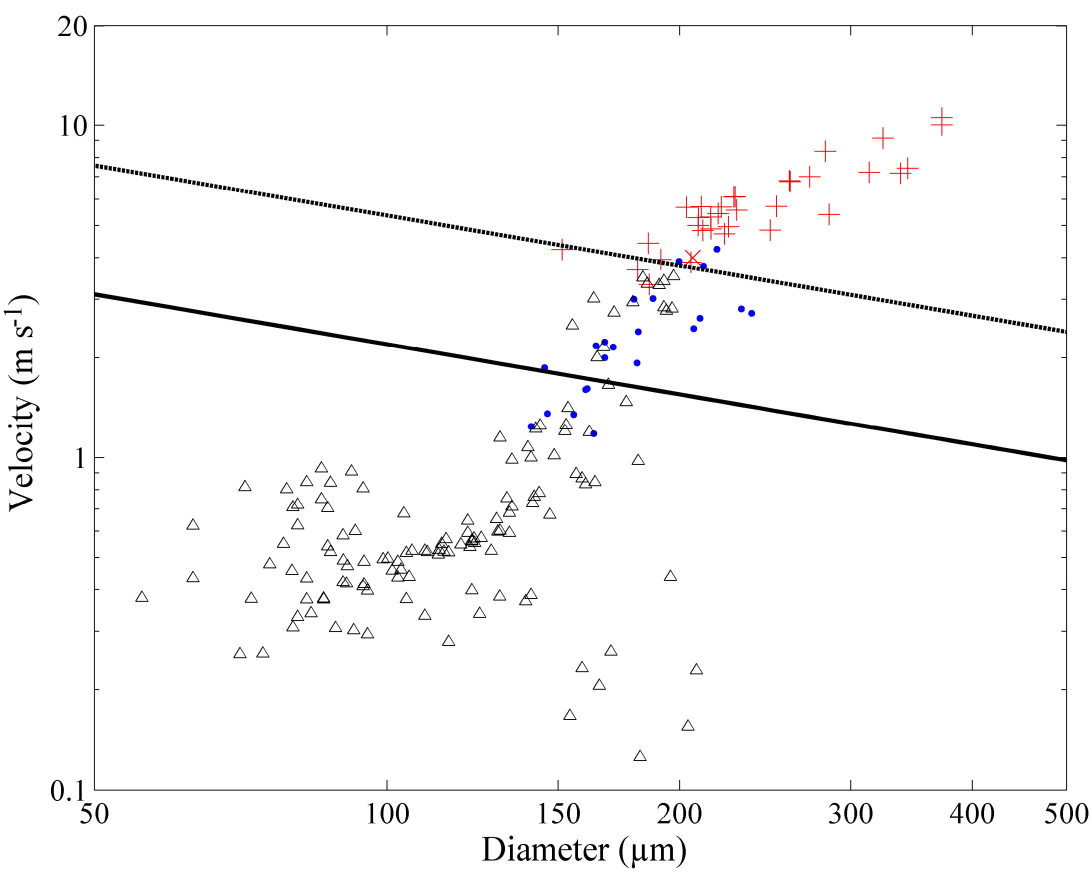

Fig. 8: Impact outcomes on the superhydrophobic slide for 0.025 (% V/V) Break-Thru® surfactant in distilled water at 0.3 MPa (Teejet 11003 nozzle at 0.5 m height): Δ adhesion, ● rebound, × pinning fragmentation, + complete fragmentation, —— Weber number of transition between adhesion and rebound (*We* = 21), - - - Weber number of transition between rebound and fragmentation (*We* = 125).

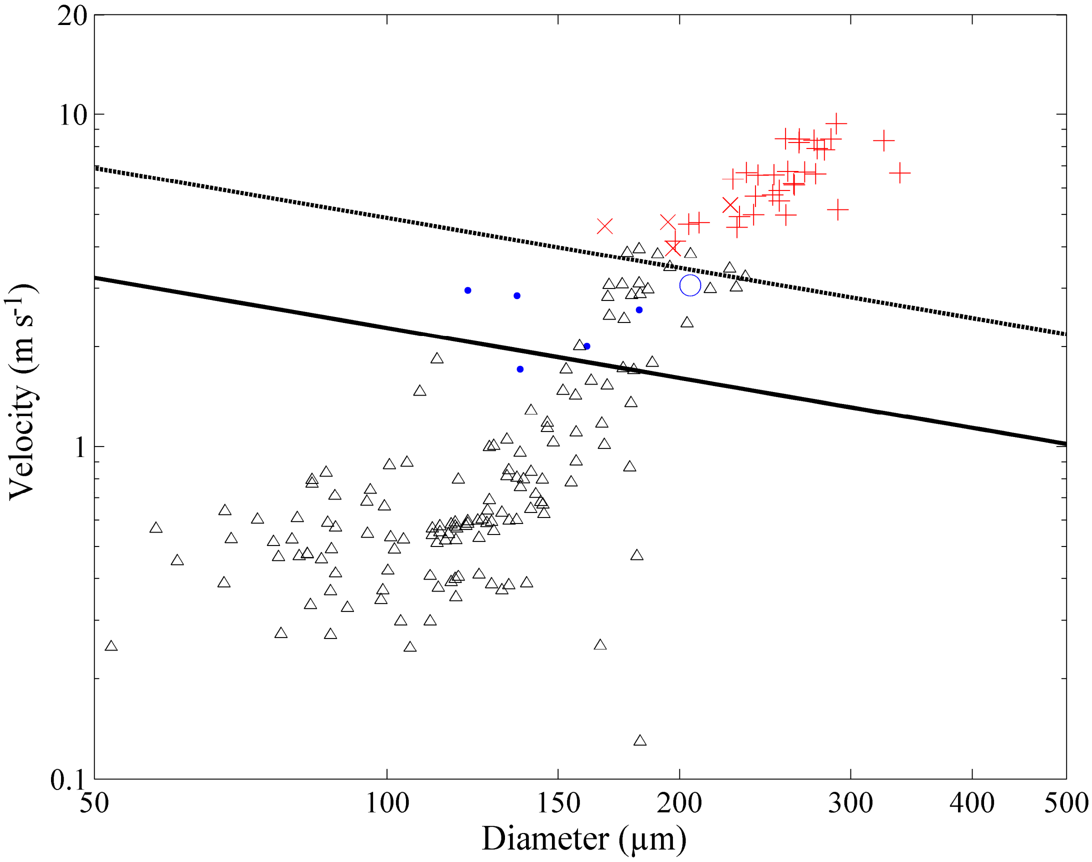

Fig. 9: Impact outcomes on the superhydrophobic slide for 0.05 (% V/V) Break-Thru® surfactant in distilled water at 0.3 MPa (Teejet 11003 nozzle at 0.5 m height): Δ adhesion, ● rebound, ○ pinning rebound, × pinning fragmentation, + complete fragmentation, —— Weber number of transition between adhesion and rebound (*We* = 24), - - - Weber number of transition between rebound and fragmentation (*We* = 110).

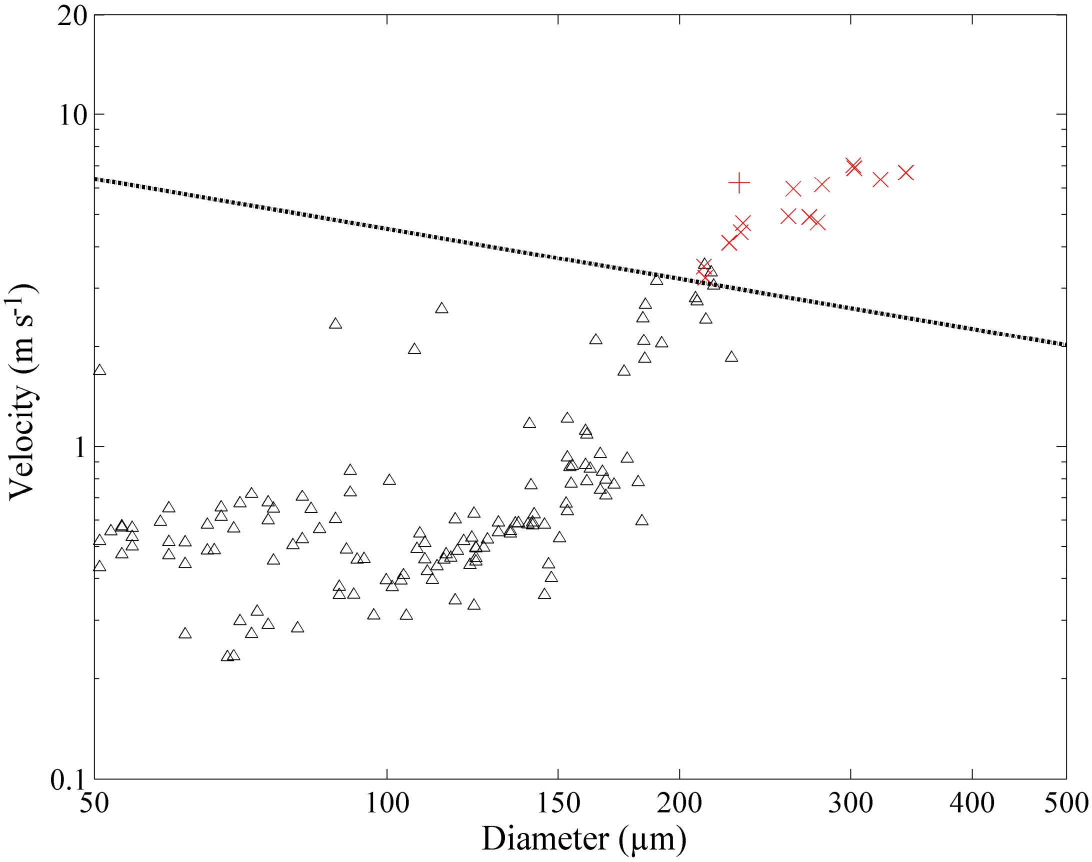

Fig. 10: Impact outcomes on the superhydrophobic slide for 0.1 (% V/V) Break-Thru® surfactant in distilled water at 0.3 MPa (Teejet 11003 nozzle at 0.5 m height): Δ adhesion, ● rebound, × pinning fragmentation, + complete fragmentation, - - - Weber number of transition between adhesion and fragmentation (*We* = 95). Drop rebound totally vanishes and pinning fragmentation replaces complete fragmentation.